SIZE AND BODY CONDITION OF SOUTHERN RESIDENT KILLER WHALES

John Durban, Holly Fearnbach, Dave Ellifrit and Ken Balcomb

Center for Whale Research, 355 Smuggler's Cove Road, Friday Harbor, WA 98250, USA
John.Durban@Whaleresearch.com

February 2009

Contract report to the Northwest Regional Office, National Marine Fisheries Service
Order number AB133F08SE4742, Requisition Number NFFP5000-8-43300

Summary

The endangered southern resident population of killer whales has been shown to be food limited, and the reduced availability of their primary prey, chinook salmon, has been identified as a key threat to population viability. Our study aimed to collect aerial photogrammetry data on size and body condition, to evaluate the potential of this tool for future monitoring of individual growth and nutritional status within this population. A key feature of our approach was using our long-term photo-identification catalogue to match measurements to individual whales of known age and sex, and aerial photographic surveys were directed in real-time by boat-based whale identification to maximize the coverage of different individuals within the population.

A chartered helicopter was used to conduct 10 flights in September 2008, resulting in 2803 images from which useable measurements were possible for whales of known identification, comprising measurements from 69 individual whales from all three pods (24 J-Pod, 19 K-Pod, 27 L-Pod), representing more than three-quarters of the population. Consistent and precise estimates of the length of research vessels of known size (and approximate whale size) served as an effective ground-truthing of this technique, with an average bias of just 7cm (1.2%).

Estimated whale lengths ranged from 2.74m for a neonate whale in its first year of life (K42) to a maximum of 7.25m for a 31 year-old adult male (L41). The size of adult males >20 years old (average = 6.76m, range = 6.46-7.25m) was significantly larger than adult females >15 years old (average = 6.01m, range = 5.50 - 6.44m), with no overlap between the two ranges and an average difference of 75cm. The asymptotic length-at-age curves for both males and females indicate the consistency and accuracy of our measurement approach, and highlight its utility for detecting changes in growth through repeated longitudinal monitoring.

Estimates of breadth (at the anterior insertion of the dorsal fin) ranged from 13% to 18% of the total body length for different whales (average = 15%), with the largest proportional breadth estimated from the neonate K42 that was still nursing. Estimates of head width (behind the cranium) ranged from 10% to 17% of body length (average = 13%), with this larger between-whale variability showing greater potential for assessing body condition. Variability in head widths was driven mainly by notably large proportional head widths for young calves: the neonate K42 had the maximum estimated head width of 17% of the estimated body length. Conversely, the mother of K42 (K14) had the smallest head width to body length ratio (10%), likely indicating a decrease in body condition due to the energetic burden of lactation. The female with the second smallest head width was L67 (age 23), who's head was thinner than all other adult females. This whale was documented from boat-based photographs to be in very poor body condition, with a pronounced depression behind the cranium, and she was measured on the last day that she was documented by CWR (presumed dead). These data indicate the potential of aerial photogrammetry to detect changes in body condition. However, judging of the utility of this approach for assessment of nutritional status requires further monitoring to assess the variability across repeated longitudinal measurements from the same whales, particularly between seasons and across years.

Background

Reduced food availability has been identified as a key threat facing the endangered southern resident killer whale (*Orcinus orca*) population. Demographic analysis of long-term photo-identification data has shown this population to be food-limited, with a highly significant correlation between the survival probability of individuals and the abundance of chinook salmon (*Oncorynchus tshawytscha*) retuning to rivers in the Pacific Northwest (Ford, Ellis and Olesiuk, 2005). Similarly, recent analysis of individual association patterns has also demonstrated a reduction in social cohesion in the years with low chinook availability (Parsons et al. in press). Our study aimed to support and extend the individual-based monitoring of the status of the southern resident killer whale population by collecting aerial photogrammetry data on size and body condition.

For long-lived marine mammals, data on body condition and individual growth can provide important indications of individual health and population status (Perryman and Lynn 2002). We have developed and tested a novel approach for obtaining morphometric measurements using laser-beam pointers (Durban and Parsons, 2006), that is being routinely implemented alongside photo-identification studies conducted from small boats. However, it has not been possible to measure total body length, due to submerged portions of the whale. Similarly, breadth measurements are unavailable, and these may be particularly useful for assessing changes in body condition.

In order to estimate body length and breadth, this study used a helicopter platform to obtain high-quality images from directly above whales. We used proven photogrammetric techniques for providing precise measurements (Perryman and Lynn 2002), which have recently been successfully used to measure body lengths of killer whales in the Antarctic (Pitman et al. 2007). A key feature of our approach was using the Center for Whale Research (CWR) long-term photo-identification catalogue to match measurements to individual whales of known age and sex, and aerial photographic surveys were directed in real-time by boat-based photo-identification surveys to maximize the coverage of different individuals within the population

Approach

We chartered a Robinson R44 Clipper helicopter (Figure 1) to survey for whales from a base at Friday Harbor airport during September 2008. To minimize search time, flights were only conducted on days when southern resident killer whales had been reported to be in the area, and the CWR research boat had established contact with the whales. Guided by communications from the boat, the helicopter searched for whales at an altitude of around 1000ft (~305m), with decents to as low as 750ft (~229m) to photograph whales. All approaches below 1000ft were conducted under the authority of a National Marine Fisheries Service permit issued to CWR (#532-1822) to conduct aerial surveys of southern resident killer whales under the Endangered Species act and Marine Mammal Protection Act.

Figure 1: The Robinson R44 clipper helicopter used to obtain aerial photogrammetric images, with the pilot (forward) and photographer (rear) leaning out of the open doors to spot surfacing whales.

One of the authors (JD) acted as an onboard guide to the helicopter pilot, continuously using communication from the research boat to direct the helicopter over target whales. In this way, visual identifications of individual whales by a highly experienced observer (DE) aboard the research boat were used to efficiently move the helicopter to different individuals to maximize coverage of the population. The helicopter then hovered to hold position over each target whale until the photographer (HF) had captured suitable images of the whale. The photographer was positioned in the passenger seat behind the pilot so that both could obtain a similar view which facilitated positioning directly overhead of the whale.

Wearing a seat harness, the photographer then leaned out of the open passenger door to shoot photographs vertically down on the target whale. A bubble-level was attached to the back of a hand-held digital SLR camera (Nikon D300), to ensure that the camera was orientated vertically, while the photographer used a motor-drive to capture as many images as possible of the surfacing whale. Photographs were taken when the whale was at the water surface and parallel to the water surface. High quality JPG images were shot at a resolution of 4288 x 2848 pixels (13.1 Megapixel resolution) in preference to RAW images in order to maximize the number of frames per second (to approximately 6fps). This ensured that the most elongated position of the whale was captured on each surfacing. A fixed focal length 180mm f2.8 AF Nikkor lens was used either with or without a 1.4x Kenko Pro extender, to achieve a realized focal length of either 378 or 270 mm (after accounting for the focal length factor of 1.5 inherent in the digital image sensor of the camera).

The altitude was recorded at one second intervals throughout each flight using an onboard Garmin GPSMap 396 aerial GPS. This WAAS-enabled differential GPS continuously received parallel signals from 12 satellites, and also calibration signals from shore-stations, to compute and update the position with precision to less than 3m. The GPS and camera time were synchronized so that each image could be linked to a specific altitude using a relational database. To ensure that these two time stamps were precisely matched, a Blue2Can Bluetooth receiver on the camera received wireless time signals from a second GPS (Holux M241), and this time was directly embedded into the metadata associated with each image. This ensured that both the altitude-linked aerial GPS time and the camera time were both derived from GPS signals, rather than relying on the pre-set camera clock that had to be manually updated.

Prior to measuring, every photograph was examined by one of the authors (DE) who has unprecedented experience and ability in identifying individual southern resident killer whales. Photographs were displayed on a 22-inch high-resolution flat panel monitor, using ACDSee photo manager. Photographs were linked to known individuals (of known age and gender class) by matching whales to the long term (33-year) CWR identification catalogue, using saddle patch pigmentation patterns (Figure 2). These matches were validated where possible by examining identification photographs obtained during the coordinated boat-based operations, and also using boat-based records of group composition and spacing.

Figure 2: Left and right side identification photographs obtained from boat platforms (left) of L78, a male born in 1989,displaying the distinctive saddle patch pigmentation used to confirm identification from aerial images (right).

Photographs of identified whales were then re-examined by one of the authors (HF) for measurement purposes, again using a 22-inch high-resolution monitor. ACDSee photo manager was first used to perform a second check of the individual identities by cross referencing the identification catalogue, and then to select the best image(s) from each surfacing sequence of an identified whale. A quality filter was used to select only images that were deemed to be vertical and with the whale in straight orientation (i.e. body axis of the whale was not tilted), and the most elongated image(s) of each whale was then selected from the filtered set from each surfacing. The freely available software ImageJ was used to measure the distance (in pixels) between the tip of upper jaw to the notch in the flukes (*length*) and the width of each whale at the anterior insertion of the dorsal fin (*breadth*), which was more easily defined than the posterior insertion of the dorsal fin. An additional measurement of *head width* was also made, as historical observations have shown that whales in very poor body condition have displayed notable depressions behind the cranium (a condition referred to as “peanut-head”). To define a consistent point for measuring head width, we examined aerial photographs of a number of whales to identify the posterior boundary of the cranium, including the most useful images from an adult female (L67) that was in very poor body condition and has subsequently disappeared from the population (assumed dead). Based on these images, we selected to measure at a point that was posterior to the blowhole by a distance of 15%

of the total distance between the blowhole and the anterior insertion of the dorsal fin (Figure 3).

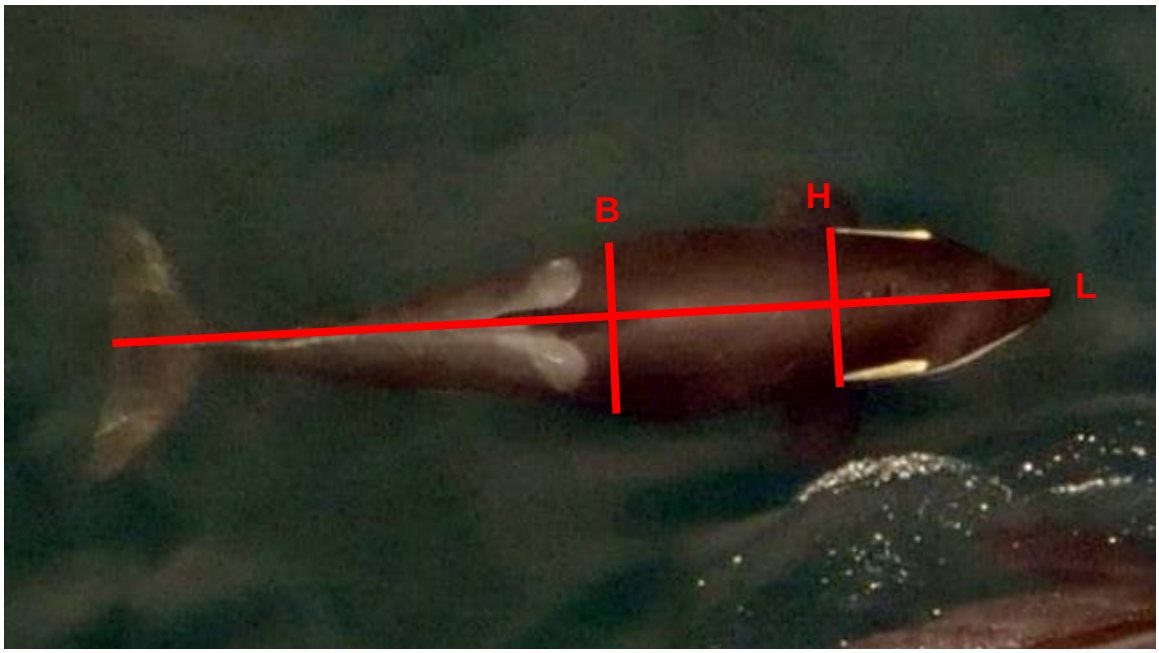

Figure 3: Illustrating the measurements of length (L, horizontal line), breadth (B, vertical line) and head width (H, vertical line) made from each aerial photograph where possible.

All measurements in pixels were first converted to a true measurement based on the actual width of the digital sensor (0.036m), and the dimensions of this sensor width in pixels (4288). These measured distances were then converted to true lengths based on the scale of each image, which can be calculated from the known altitude and realized lens focal length (scale = altitude / focal length). Images and associated data on individual identification, focal length, and size measurements were imported into a Microsoft Access database where they were linked to the GPS data on altitude based on the date and time matches. Queries were written to perform “automatic” calculations of size and data summaries.

Results

Aerial photographs were collected during 10 flights in September 2008 (Table 1). Flights lasted an average of 77 minutes (min = 61, max = 118), and whales were typically encountered in Haro Strait off the west side of San Juan Island (Figure 4).

Table 1: Summary of the 10 flights on which aerial photographs were obtained

Date	Pods Photographed	Location Encountered
08-Sep-08	J	Haro Strait
09-Sep-08	J, L	Haro Strait
11-Sep-08	J, K, L	Haro Strait
12-Sep-08	J, K, L	Eastern Juan de Fuca Strait
13-Sep-08	L	Southern Rosario Strait
14-Sep-08	J, K, L	Swanson Channel
15-Sep-08	J, K, L	Haro Strait
16-Sep-08	J, K, L	Haro Strait
18-Sep-08	J, K, L	Haro Strait
25-Sep-08	J, K, L	Boundary Pass

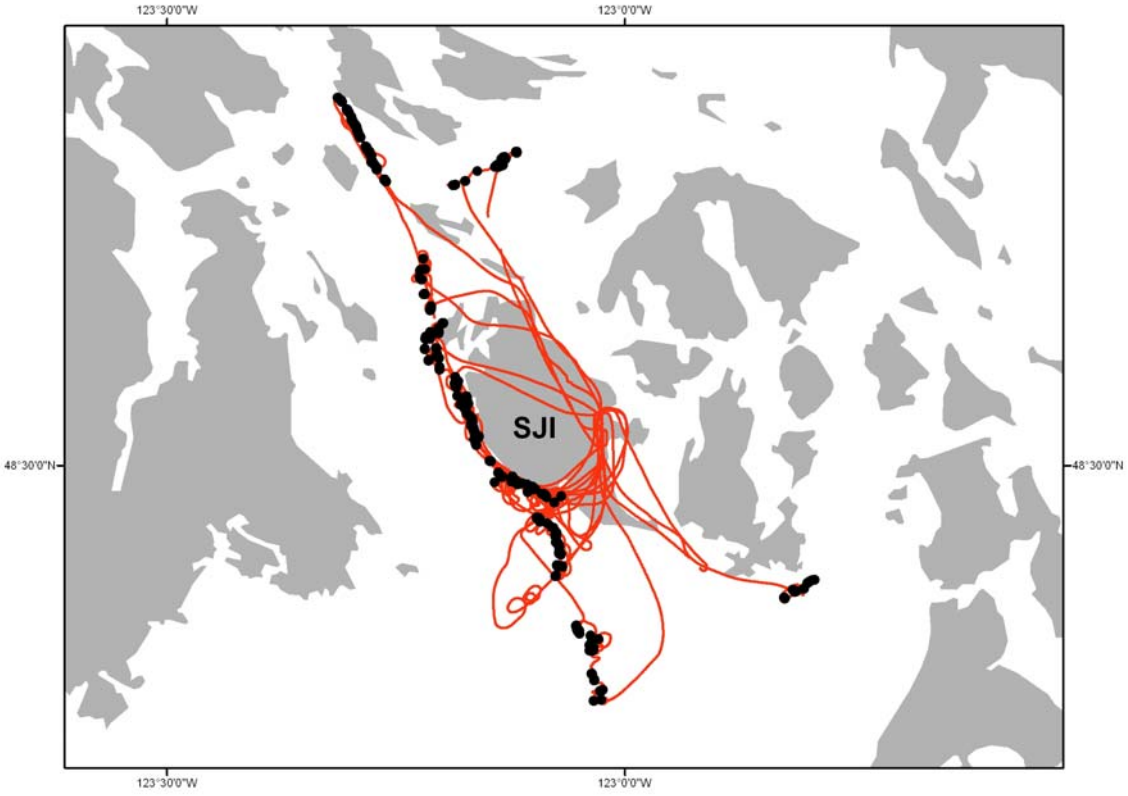

Figure 4: Map showing the tracks of the helicopter (red lines) and the locations where measurement photographs were obtained (black dots) during the 10 photogrammetry flights from San Juan Island (SJI), Washington State.

Testing on boats of known length

To test the variability in our technique, we used aerial photographs to estimate the size of boats of known-length. To be consistent with the whale measurements, we used two CWR research vessels, which were photographed in the same locations and at the same time as photographic encounters with whales. Conveniently, these boats were the same approximate size as whales from this population (see later results). These boats varied in size – one being a rigid hulled inflatable boat (RHIB) that measured 5.46m from the tip of the bow to the back of the outboard engine, and the other being a Boston Whaler measuring 6.50m for the same distance. At least one of the boats was photographed on each of 9 of the 10 total flights, with both boats being photographed on one flight, resulting in 147 measurable photographs.

There was some variability between length estimates of the same boat within days (Figure 5), but this improved across days as we quickly became better at positioning directly overhead of the research vessel, and selectively taking only vertical photographs. The maximum measurement for each boat was taken as the best estimate for that boat on each day, as smaller estimates were due to foreshortening as a result photographs taken when the boat was not directly under the helicopter. These estimates ranged from 5.41 to 5.57m across days for the RHIB and 6.22 to 6.59m for the Whaler, representing an average bias of just 0.06m (range = 0.02 – 0.10m) for the RHIB and 0.08m (range 0.00 to 0.28m) for the Whaler, which represented an average of just 1.1% of the true length (range = 0.3-1.9%) and 1.3% (range = 0.0 – 3.2%) for each of the boats respectively, and a combined average of just 1.2% (Figure 6). These consistent and precise estimates of the length of known-sized research vessels of approximate whale size served as an effective ground-truthing of this technique, suggesting that whale size estimates have the same accuracy.

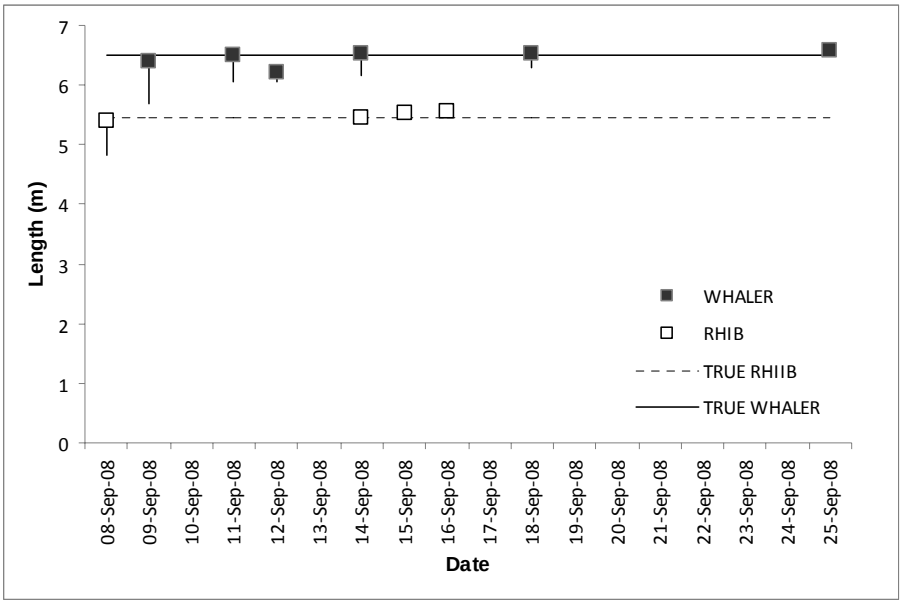

Figure 5: Length estimates for the two CWR research vessels, a 5.46m RHIB and 6.50m Boston Whaler on 9 different survey days. Squares represent the best (maximum) estimate on each day, vertical lines represent the extent of the variability between estimates within days, and horizontal lines represent the true size.

Measurements of whales

Almost three thousand (2803) images were obtained from which useable measurements were possible for whales of known identification. This set comprised measurements from 69 individual whales from all three pods (24 J-Pod, 19 K-Pod, 27 L-Pod), representing more than three-quarters of the population.

Lengths

Length estimates were possible for 66 different individuals. The estimated length generally decreased with the increasing numeric identification number within each pod (Figure 6): this was to be expected as higher identification numbers have typically been assigned to more recent births (with rare exceptions – see K40, who was previously L40).

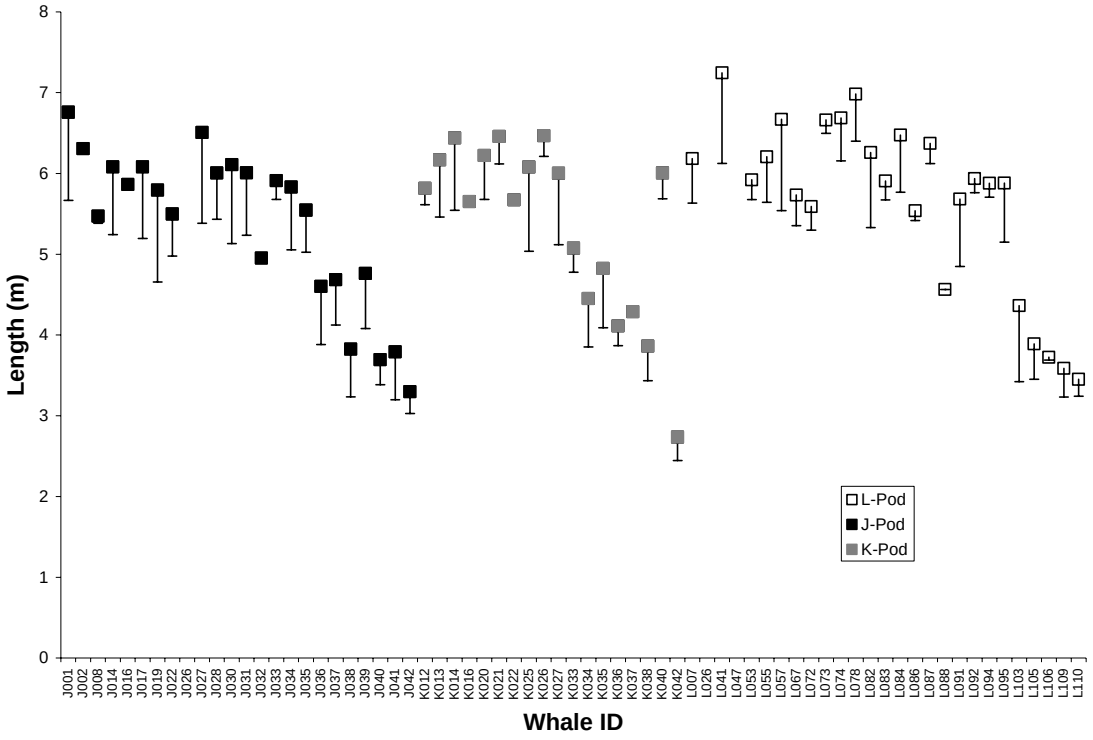

Figure 6: Length estimates for 66 different individuals from J, K and L pods within the southern resident killer whale population. Squares represent the best (maximum) estimate for each whale, vertical lines represent the extent of the variability between estimates of the same whale.

The variability within estimates of the same whale was likely due to a foreshortening effect of whales not being directly underneath the photographer, but also due to surfacing whales not being at their most elongated body position at the time of the photograph. The main bias was therefore likely to be negative, resulting in underestimates of length, and we thus chose to use the maximum estimate to be the best (least biased) for each whale. It should be noted, however, that even the maximum estimate may still have been negatively biased for full body length, and simply

represented the longest body position measured for that whale. To reduce this effect, we only considered estimates to be reliable if measurements had been obtained from at least 5 different images. All further analysis was based solely on 46 whales for which this was the case.

Estimates of length showed an asymptotic relationship with age, for both males and females, illustrating growth in body length through the mid teen years for females and the late teens for males (Figure 7). Estimated lengths ranged from 2.74m for a neonate whale in its first year of life (K42) to a maximum of 7.25m for a 31 year-old adult male (L41). These asymptotic size-at age relationships indicate the consistency and accuracy of our measurement approach, and highlight its utility for detecting changes in growth through long-term monitoring.

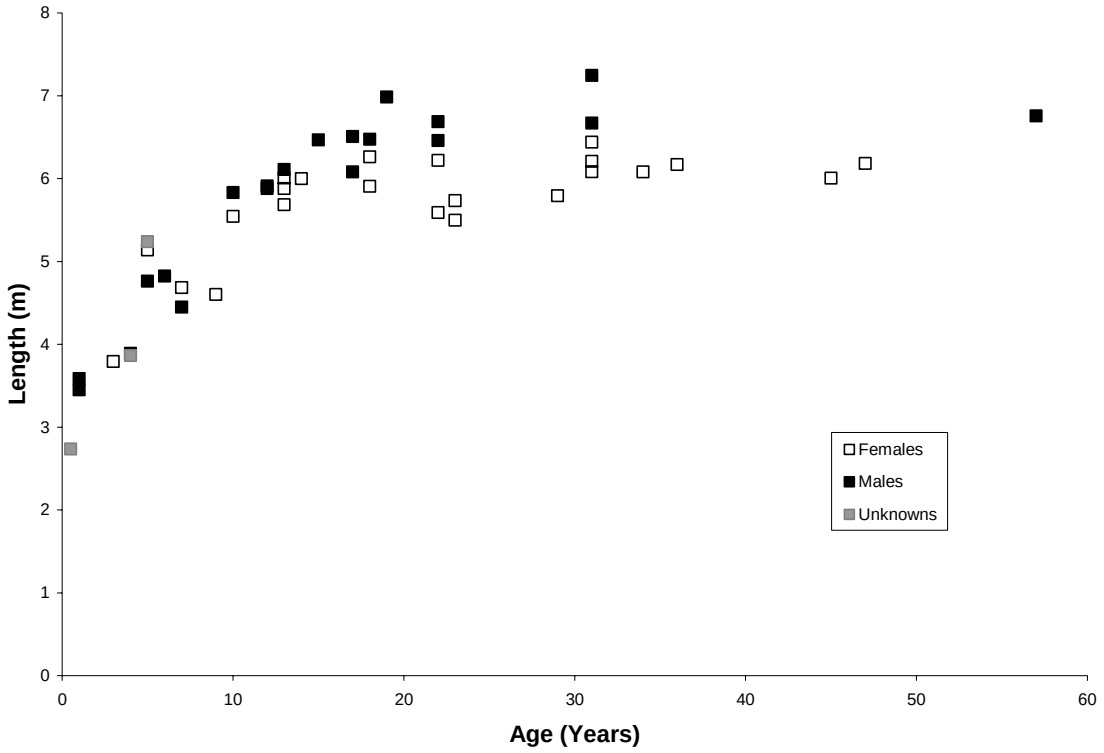

Figure 7: The maximum estimate of length for whales with five or more measurement photographs, plotted against their observed or estimated ages. Ages were estimated as per Olesiuk et al. (1990).

The average of the maximum measured size of adult males (>20 years old, following Olesiuk et al. 1990) was 6.76m (range = 6.46m [K21, age 22] to 7.25m [L41, age 31]), compared to an average of 6.01m for adult females greater than 15 years old (range = 5.50m [J22, age 23] to 6.44m [K14, 41 years]). Note that based on the maximum length estimates for each whale, there was no overlap in the size range for adult males and females, with males being significantly larger by an average of 0.75m. It is also noteworthy that some sub-adult (teenage) males attained adult body length, exemplified by L78 (6.98m), who was the second largest whale measured in this study despite being just 19 years of age at the time.

Breadths and Head Widths

Breadths and head width measurements were possible for 59 different whales. As with the lengths, the estimated breadth and head widths generally decreased with increasing numeric identification number (~ decreasing age) within each pod (Figures 8 and 9). There were some whales that were noticeably larger than the trend: L41 for breadth; J1 and L41 for head widths. For these width measurements the sources of variability were different to those involved in length measurements, as we were measuring on a different (perpendicular) axis to the length measurements. In the case of widths, any tilt in the body axis would have led to body depth (height) being measured rather than width, which could lead to a positive bias in width estimates. As a result, we considered the minimum estimate to be the best indication of true breadth and true head widths. To reduce any bias, we attempted to not photograph or measure any whales that were clearly tilted in the image, but it should be noted that even the minimum estimates may still have been negatively biased.

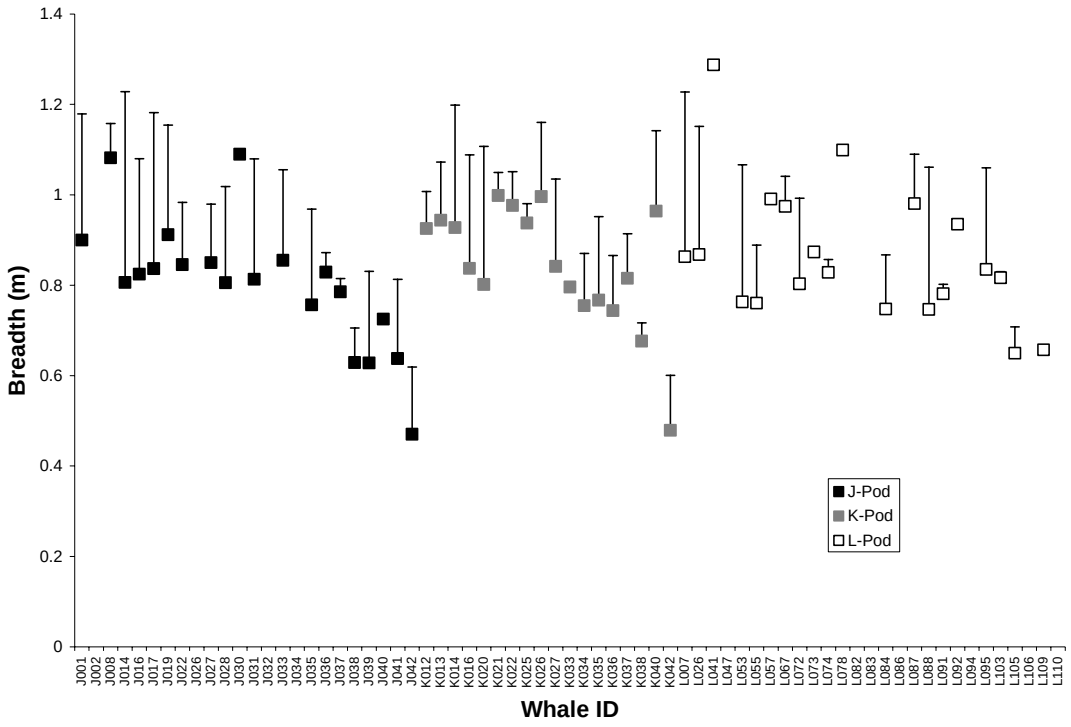

Figure 8: Estimates of breadth at the anterior insertion of the dorsal fin for 59 different individuals from J, K and L pods within the southern resident killer whale population. Squares represent the best (minimum) estimate for each whale, vertical lines represent the extent of the variability between estimates of the same whale.

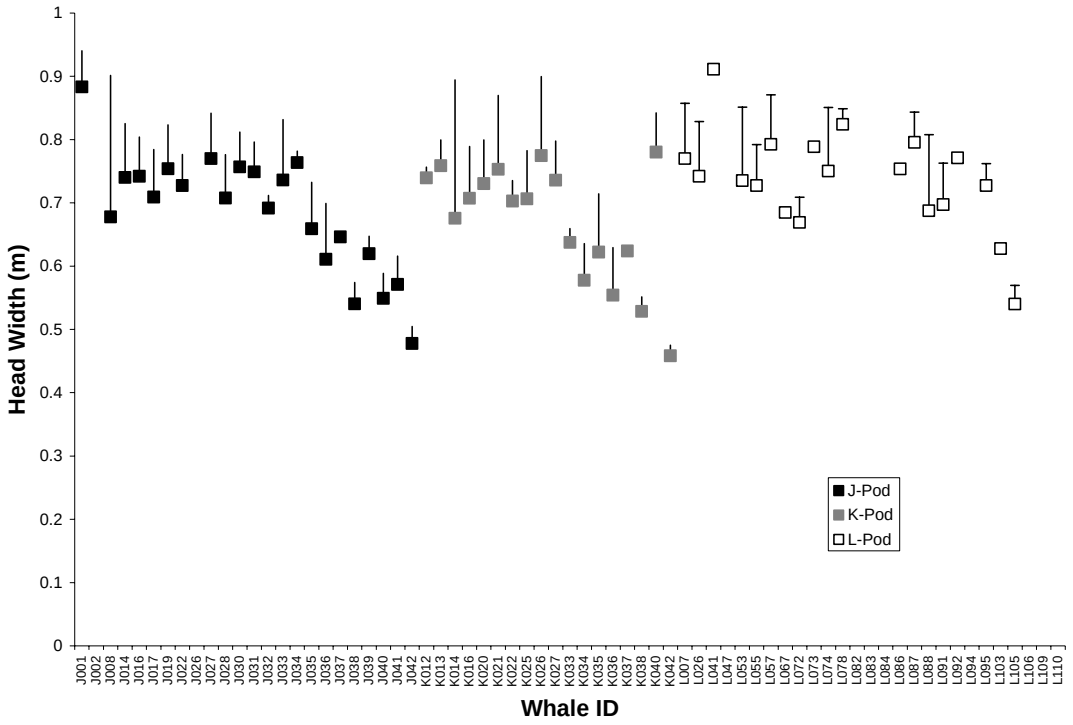

Figure 9: Estimates of head width behind the cranium for 59 different individuals from J, K and L pods within the southern resident killer whale population. Squares represent the best (minimum) estimate for each whale, vertical lines represent the extent of the variability between estimates of the same whale.

There was notably less within-whale variability when measuring head-widths in contrast to breadths, which suggests that this metric may be more useful for detecting growth and changes in body condition. This is likely due to difficulties in defining the margins of the animal at the waterline for the breadth measurements, and because the shape of the animal changes with different surfacing patterns. This appeared less of a problem for the head width, as the head was generally just below the water surface and the breaking water therefore posed less problem for defining the margins of the head.

To further reduce bias in both metrics, we only considered estimates to be reliable if measurements had been obtained from at least 5 different images (n = 30 whales). Based on this set, estimates of both breadth and head width showed tight asymptotic relationships with age, for both males and females, illustrating consistent growth in body width and head width at least through the mid teen years (Figures 10 and 11). Estimated breadths ranged from 0.47m for a one year-old whale (J42) and a neonate whale in its first year of (K42) to a maximum of 1.16m for a 15 year-old sub-adult male (K26) (Figure 10). Similarly estimated head widths ranged from 0.46 for the neonate K42 to 0.88m for an adult male (J1) estimated to be greater than of 50 years old (Figure 11).

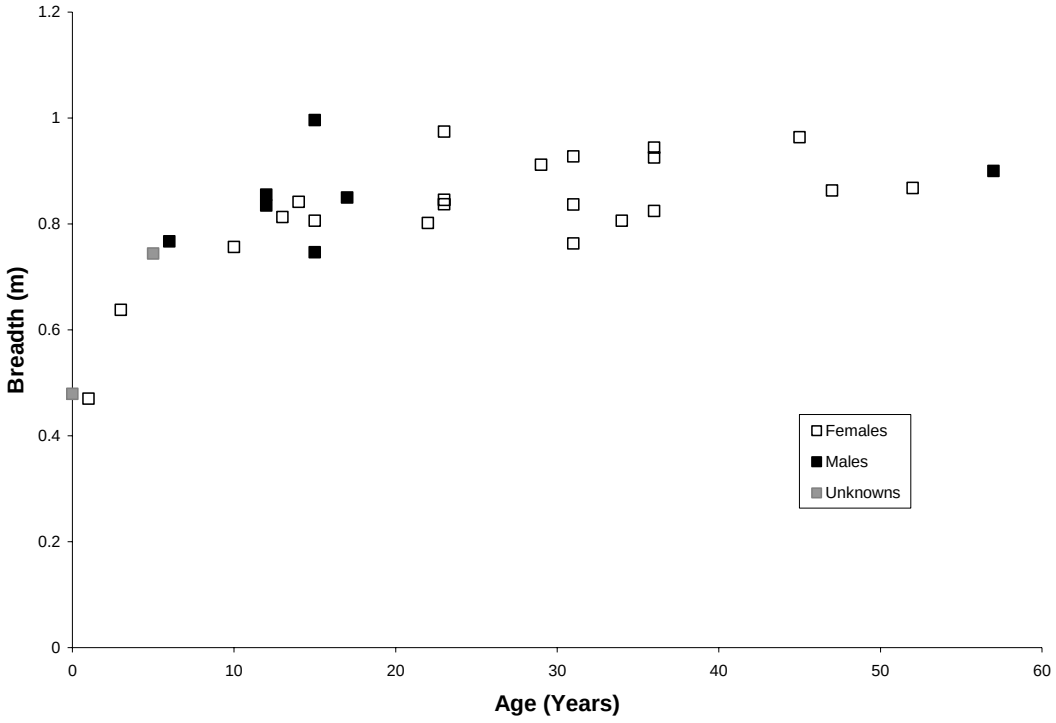

Figure 10: The minimum estimate of breadth (at anterior insertion of the dorsal fin) for whales with five or more measurement photographs, plotted against their observed or estimated ages. Ages were estimated as per Olesiuk et al. (1990).

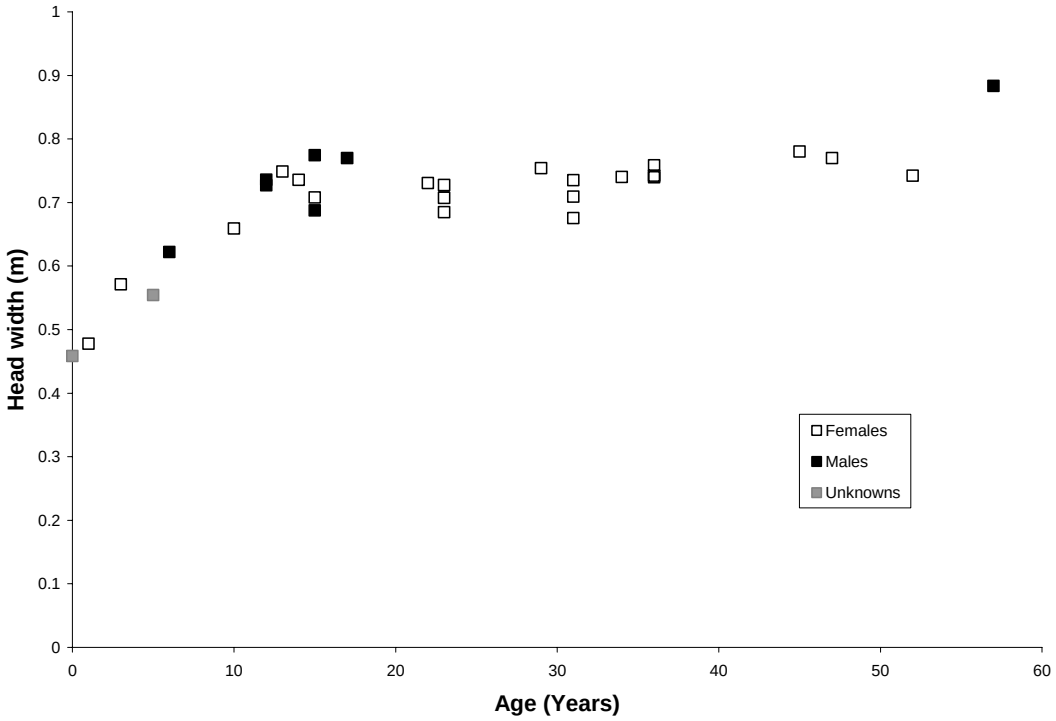

Figure 11: The minimum estimate of head width (behind the cranium) for whales with five or more measurement photographs, plotted against their observed or estimated ages. Ages were estimated as per Olesiuk et al. (1990).

To investigate if these width measurements could be used to provide an index of body condition, we calculated the best estimate (minimum) of breadth and head width for each whale as a proportion of the best estimate (maximum) of its total length, for whales from which has had obtained at least five measurements of each metric. Estimates of breadth ranged from 13% to 18% of the total body length (average = 15%), with the largest proportional breadth estimated from the youngest animal (first year K42) that was still dependent on nursing. However, there were no obvious outliers, perhaps partly due to a masking effect of the large within-whale measurement variability that may have constrained our ability to detect between-whale differences (Figure 12).

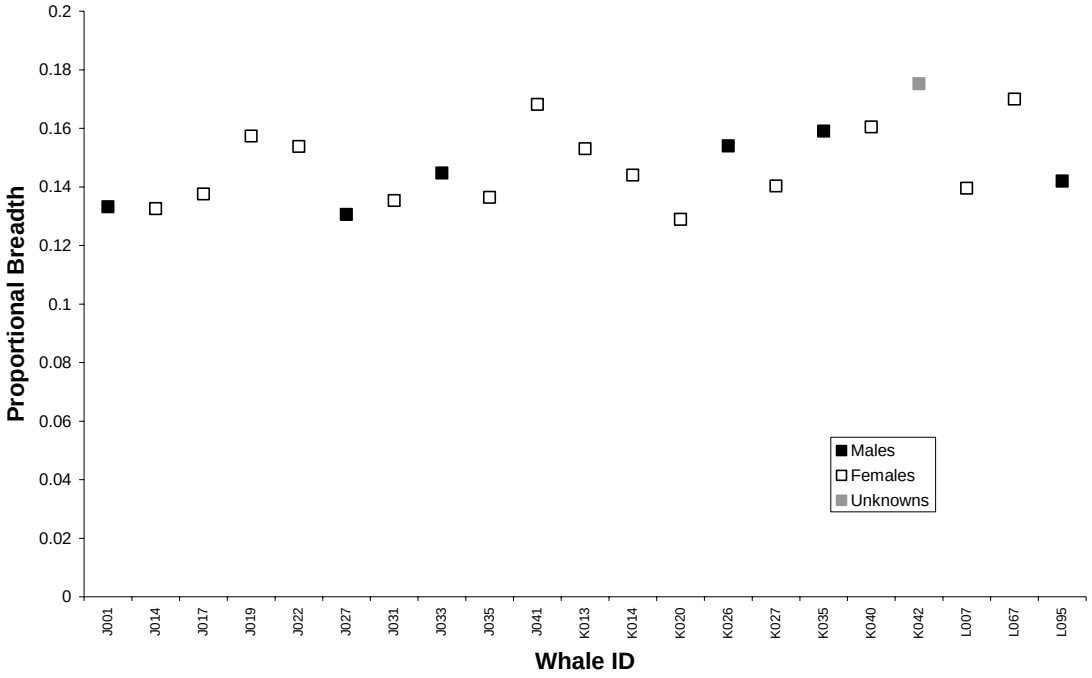

Figure 12: The best (minimum) estimates of breadth (at anterior insertion of the dorsal fin) each individual with five or more breadth measurements expressed as a proportion of the best (maximum) estimate of body length.

Estimates of head width ranged from 10% to 17% of body length (average = 13%), with this larger between-whale variability showing greater potential for assessing body condition than did breadths (Figure 13). Variability in head widths was driven mainly by notably large proportional head widths for young calves: the neonate K42 had the maximum estimated head width of 17% of the estimated body length and the second largest head width proportion was 15% for the second youngest whale with available head width measurements (J41, 3 years), which may still have been nursing.. Conversely, the mother of K42 (K14) had the smallest head with to body length ratio (10%), likely indicating a decrease in body condition due to the energetic burden of lactation. This indicates the potential of aerial photogrammetry to detect changes in body condition.

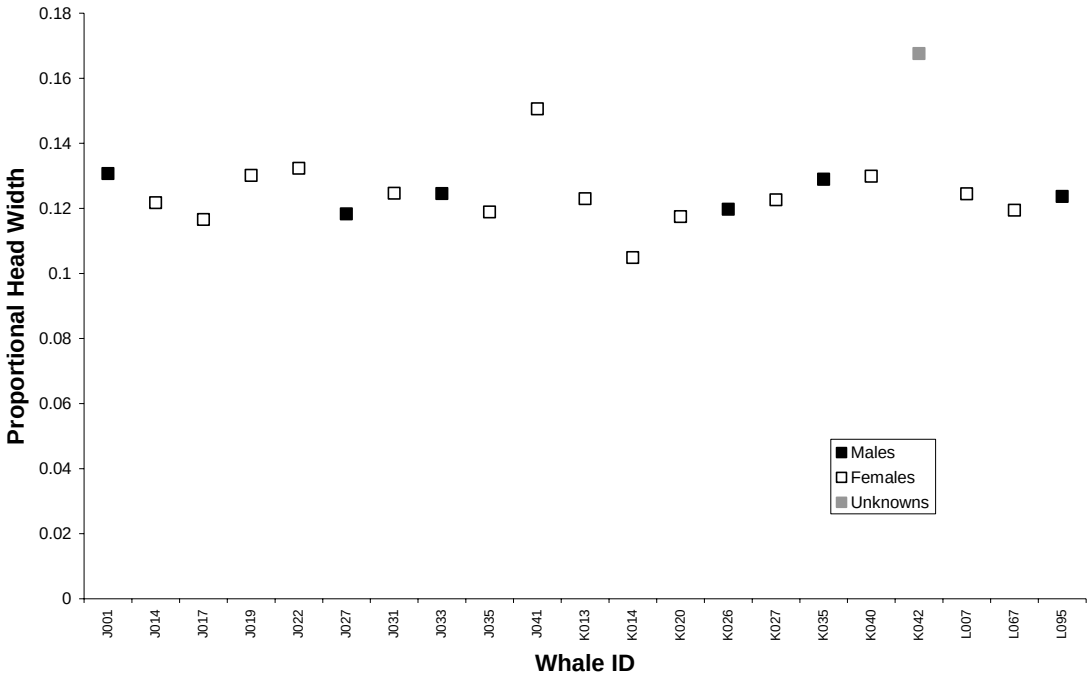

Figure 13: The best (minimum) estimates of head width (behind the cranium) each individual with five or more head width measurements expressed as a proportion of the best (maximum) estimate of body length.

Notably the breadth and head width proportions did not provide resolution for detecting poor body condition of one particular female (L67, 23 year-old female) that was determined from boat-based observations to be in very poor body condition, with a notable depression behind the cranium. This whale was last seen by CWR (and documented in aerial photographs) on 13th September 2008 and subsequently disappeared from the population (presumed dead). The lack of resolution in our proportion estimates for documenting L67's condition indicates that these proportions may not be the most appropriate indicators of body width. Specifically, L67 is shorter than average adult females, with a maximum length estimate of 5.73m compared to the average of 6.01m for adult females (range = 5.50 – 6.44m). This led to relatively high estimates of proportional body width, even though the actual widths may have been reduced due to poor body condition. When we just considered the best (minimum) estimates for the absolute head width of all adult females (>15 years old), we revealed that L67's head width was smaller than every other female except for K14, the lactating mother of the neonate K42 (Figure 14).

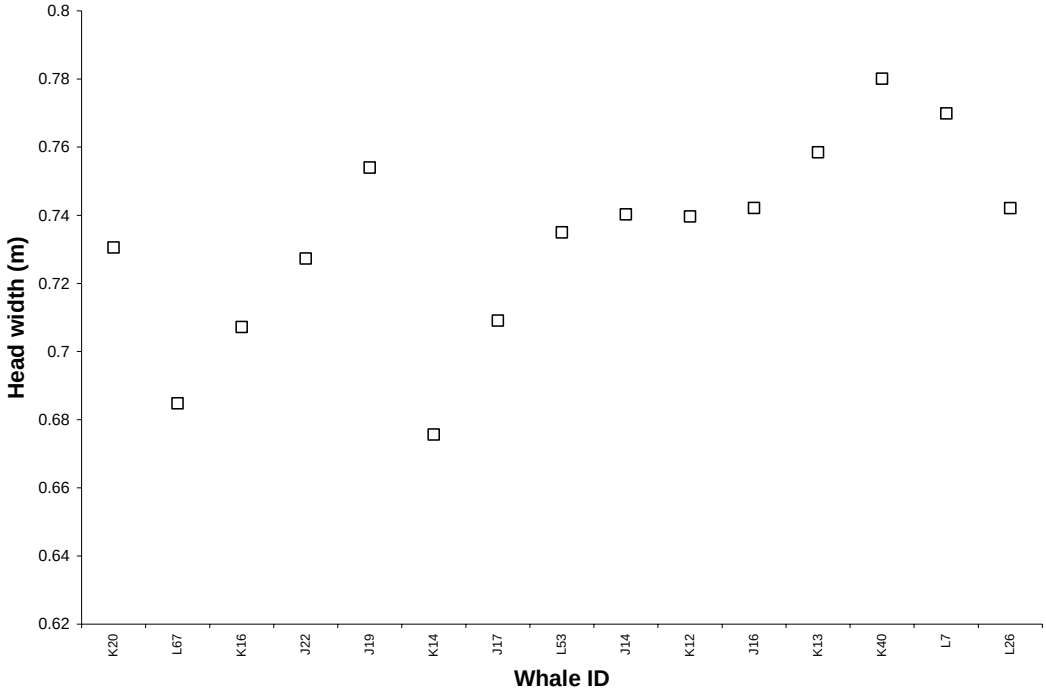

Figure 14: The best (minimum) estimates of head width (behind the cranium) for each adult female (>15 years old) with five or more head width measurements expressed as an absolute measure.

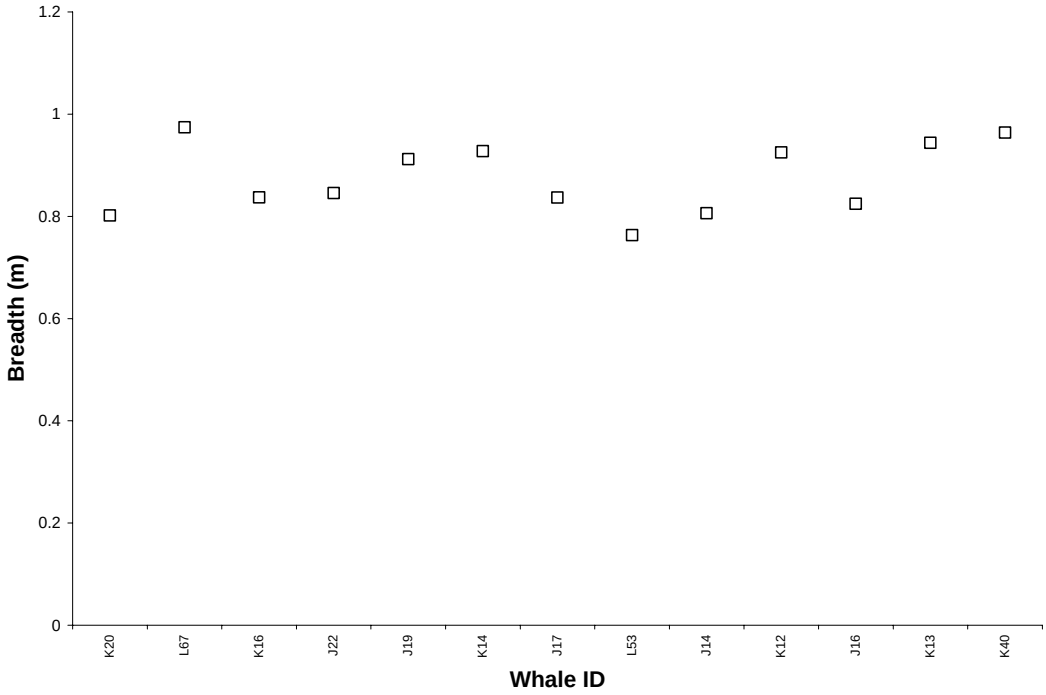

Figure 15: The best (minimum) estimates of breadth (at anterior insertion of dorsal fin) for each adult female (>15 years old) with five or more head width measurements expressed as an absolute measure.

The best estimate of head width for L67 was 0.68m compared to the adult female average of 0.73m (range 0.68 – 0.78m). Once again, there was less information on body condition from the breadth measurements, and L67 actually had the largest estimated breadth of all adult females 0.97m compared to the adult female average of 0.87m (range 0.76 – 0.97m) (Figure 15).

The disparity between the inference from proportional and absolute head widths illustrates that variability in body condition between individuals can be masked by individual variability in body proportions, and highlights that detection of changes in body condition requires repeat longitudinal measurements over time on the same individuals. Nonetheless, comparison of our measurements of body widths (particularly head width) between individuals suggests considerable utility for detecting changes in body condition.

Historical observations of body condition

The "peanut-head" condition observed in L67 has been documented by CWR on 13 previous occasions involving 13 members of the population, and all but two of these whales subsequently died. Our observations have documented that this condition is typified by a pronounced depression behind the blowhole / cranium, and the surfacing behavior of the whale can be described as a flat "ploughing" motion rather than a pronounced arched surfacing. These symptoms have been observed for the following whales at the following times:

1994

L42 **(**male born est.1973) – a slight depression behind the blowhole was first noticed in mid June 1994; a prominent depression by mid July; the dorsal fin was drooping by mid August; the depression had become large by early September exposing the shape of the back of the cranium and vertebrae; last seen in late September.

K17 (male born est.1966) – a slight depression behind the blowhole was first noticed in mid July; prominent depression by mid August; last seen in mid September with the fin severely drooping.

1995

J3 (male born est. 1953) – a slight depression behind the blowhole noticeable by the end of March; moderate depression by mid May, with the fin beginning to droop; last seen late May.

L63 (male born 1984) – a prominent depression behind the blowhole noticeable by late July; last seen late July.

L68 (male born 1985) – a moderate depression behind the blowhole was noticeable in mid may; depression prominent by mid June; last seen in late June.

1996
J12 (female born est. 1972) – a slight depression behind the blowhole first noticed in mid February; depression moderate by April with the base of the cranium apparent; prominent depression by early June, with ribs beginning to show on flanks; depression very prominent by early September, revealing the shape of the base of the cranium and vertebrae, and ribs visible on flanks showing; last seen late September.

L9 (female est. 1931) – a slight depression behind the blowhole noticeable in early July; depression prominent by mid August, exposing the shape of the base of the cranium; last seen mid August.

1997
J5 (female est. 1938) – a slight depression noticeable in early April; last seen early April.

2002
L102 (calf of unknown gender born 2002) – moderate depression behind the blowhole noticeable in early December – only time the calf was seen; last seen early December.

2005
K25 (male born 1991) – a moderate depression was noticeable behind the blowhole in late July, with a laceration on the whales back following a collision with a whale-watch boat in early July; depression slight by early September; whale survived.

2006
K28 (female born 1994) – a prominent depression behind the blowhole was noticeable in mid September; whale not seen afterwards.

2008
L106 (male born 2005) – a prominent depression behind the blowhole was noticeable in mid June; depression just slight by mid July; depression barely noticeably by early August; whale survived the year, and seen in early 2009.

L67 (female born 1985) – a slight depression behind the blowhole was first noticeable in late June; depression still slight in early August; depression prominent by mid September; last seen mid September.

These data show that boat-based photographs have been a useful too for detecting declines in body condition that have typically been terminal, because the whales only visibly deteriorate in body condition from dorsal views when their condition has become very poor.. The data presented in this report indicate that aerial photogrammetry likely provides greater resolution for monitoring changes in size and condition of individual whales: a hypothesis that can be tested by repeated photogrammetric surveys to collect longitudinal measurements of individually recognizable whales

Recommendations

Continued photo-identification: The unprecedented ability to link photogrammetric measurements to individuals of known identity, gender and age would not have been possible without the detailed knowledge of the whales, the characteristic features used for their identification, and their life histories. These data have been collected and updated by the Center for Whale Research for more than 30 years, fostering researchers that are knowledgeable about these whales and skilled in their identification. Photo-identification continues to provide the backbone of research into the ecology and demographics of this population, and should continue to be the priority for funding support. During this study, researchers skilled in identifying individual whales were able to direct the helicopter to different target individuals, allowing measurements to be obtained from more than three-quarters of the population. Further aerial photogrammetry should continue to operate with the support of experienced boat-based researchers.

Repeated aerial photogrammetry: The asymptotic length-at age relationships estimated from this study indicate the consistency and accuracy of our measurement approach, and highlight its utility for detecting changes in growth through long-term monitoring. With this aim, aerial photogrammetric surveys should be continued to monitor changes in size of identifiable individuals in a longitudinal fashion. Variability in breadth and head width also appear to be linked to overall body growth (and thus age), but appear to offer some utility (particularly head width) for detecting changes in body condition. Repeat longitudinal measurements from the same whales will enable an evaluation of measurement variability over time, which can be used examine the inherent differences in body proportions between individual whales, our ability to detect changes in body condition, and the magnitude and nature of any such changes. It would be useful to conduct surveys in different seasons (e.g. winter, early summer and fall) to examine for seasonal variability in body condition.

Further data analysis: The lack of resolution in our breadth data for documenting the pronounced deterioration in body condition of at least one whale (L67) indicates that our chosen measurement sites on the body for width measurements may not be the most appropriate indicators. We recommend that our existing data be used in a further analysis of the full width profiles at different points along the body axis to evaluate and develop more sensitive numerical summaries of body condition.

Literature Cited

Durban, J .W. and Parsons, K.M. 2006. Laser-metrics of free-ranging killer whales. Marine Mammal Science 22, 735-743.

Ford, J.K.B., Ellis, G.M. and Olesiuk, P.F. 2005. Linking prey and population dynamics: did food limitation cause recent declines of 'resident' killer whales (*Orcinus orca*) in British Columbia? Research Document 2005/042. Canadian Science and Advisory Secretariat, Fisheries and Oceans Canada. http://www.dfo-mpo.gc.ca/csas/.

Olesiuk, P.F., Bigg, M.A. and Ellis, G.M. 1990. Life history and population dynamics of resident killer whales (*Orcinus orca*) in the coastal waters of British Columbia and Washington State. Pages 209-244 *in* Reports of the International Whaling Commission. Special Issue 12.

Parsons, K.M., Balcomb, K.C., Ford, J.K.B and Durban, J.W. In Press. The social dynamics of the southern resident killer whales and implications for the conservation of this endangered population. Animal Behaviour.

Perryman, W.L. and Lynn, M.S. 2002. Evaluation of nutritive condition and reproductive status of migrating gray whales (*Eschrichtius robustus*) based on analysis of photogrammetric data. Journal of Cetacean Research and Management 4: 155-164

Pitman, R.L., W.L. Perryman, D. LeRoi, and E. Eilers. 2007. A dwarf form of killer whale in Antarctica. Journal of Mammalogy 88:43-48.

Appendix 1: Measurements of length, breadth (at the anterior insertion of the dorsal fin) and head width (behind the cranium) for whales with five or more measurements for each metric.

Whale ID	Age	Gender	Max of length	Min of breadth	Min of head width
J001	57	M	6.76	0.90	0.88
J014	34	F	6.08	0.81	0.74
J016	36	F		0.82	0.74
J017	31	F	6.08	0.84	0.71
J019	29	F	5.79	0.91	0.75
J022	23	F	5.50	0.85	0.73
J027	17	M	6.51	0.85	0.77
J028	15	F		0.81	0.71
J030	13	M	6.11		
J031	13	F	6.01	0.81	0.75
J033	12	M	5.91	0.86	0.74
J034	10	M	5.83		
J035	10	F	5.54	0.76	0.66
J036	9	F	4.60		
J037	7	F	4.68		
J038	5	U	3.82		0.54
J039	5	M	4.76		
J040	4	F			0.55
J041	3	F	3.79	0.64	0.57
J042	1	F		0.47	0.48
K012	36	F		0.93	0.74
K013	36	F	6.17	0.94	0.76
K014	31	F	6.44	0.93	0.68
K016	23	F		0.84	0.71
K020	22	F	6.22	0.80	0.73
K021	22	M	6.46		
K025	17	M	6.08		0.71
K026	15	M	6.47	1.00	0.77
K027	14	F	6.00	0.84	0.74
K034	7	M	4.45	0.75	
K035	6	M	4.82	0.77	0.62
K036	5	U		0.74	0.55
K038	4	U	3.86	0.68	
K040	45	F	6.01	0.96	0.78
K042	0	U	2.74	0.48	0.46
L007	47	F	6.18	0.86	0.77
L026	52	F		0.87	0.74
L041	31	M	7.25		
L053	31	F		0.76	0.73
L055	31	F	6.21		
L057	31	M	6.67		
L067	23	F	5.73	0.97	0.68
L072	22	F	5.59	0.80	
L074	22	M	6.69		0.75
L078	19	M	6.98		
L082	18	F	6.26		
L083	18	F	5.91		
L084	18	M	6.47		
L087	16	M		0.98	
L088	15	M		0.75	0.69
L091	13	F	5.68		0.70
L094	13	F	5.88		
L095	12	M	5.88	0.83	0.73
L103	5	F	4.36		
L105	4	M	3.89		
L109	1	M	3.59		
L110	1	M	3.45		